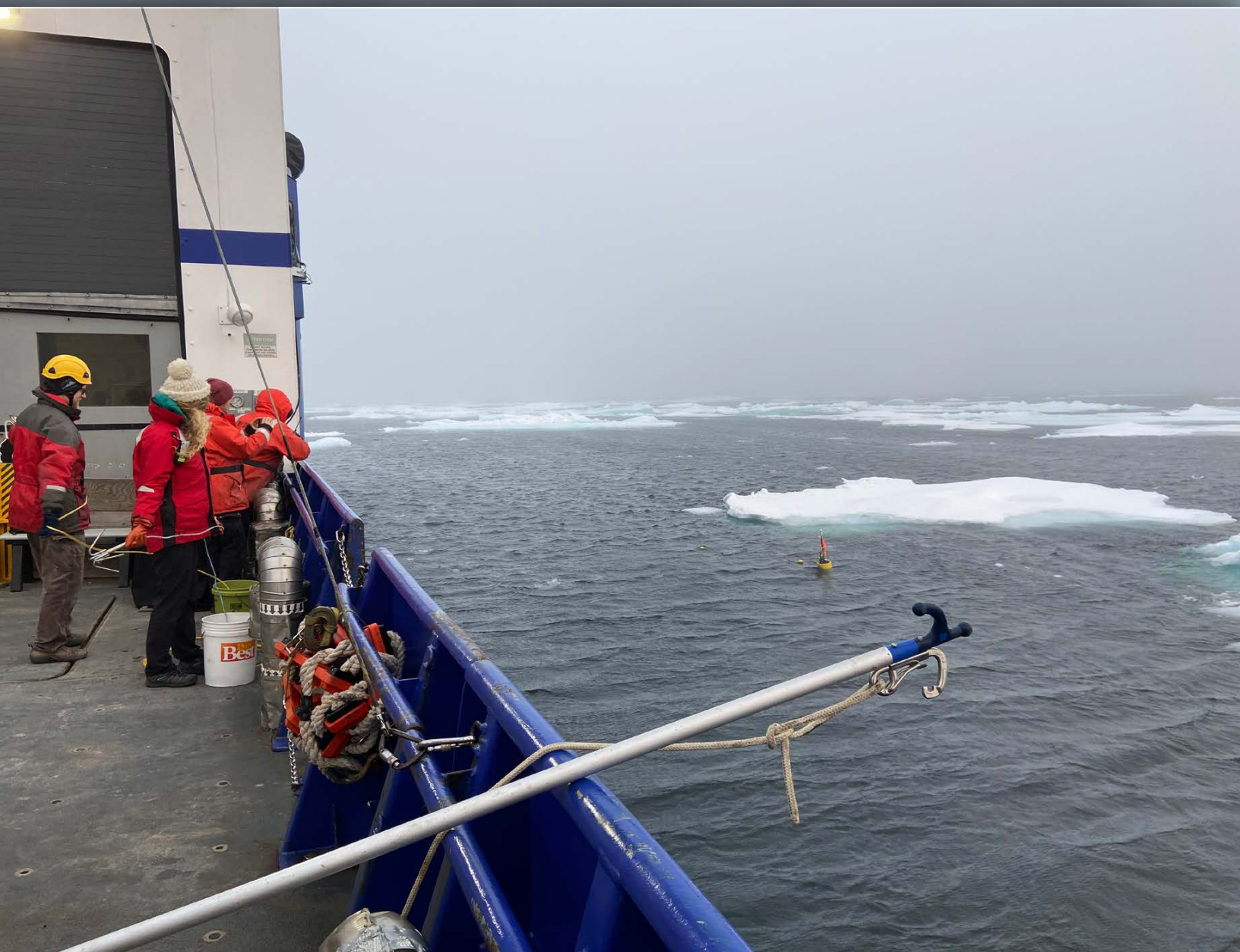# AIR-ICE-OCEAN INTERACTIONS AND THE DELAY OF AUTUMN FREEZE-UP IN THE WESTERN ARCTIC OCEAN

By Jim Thomson, Maddie Smith, Kyla Drushka, and Craig Lee

Preparing to recover a SWIFT buoy in the marginal ice zone from R/V *Sikuliaq* on September 30, 2020. *Photo credit: Alex de Klerk*

ABSTRACT. Arctic sea ice is becoming a more seasonal phenomenon as a direct result of global warming. Across the Arctic, the refreezing of the ocean surface each autumn now occurs a full month later than it did just 40 years ago. In the western Arctic (Canada Basin), the delay is related to an increase in the seasonal heat stored in surface waters; cooling to the freezing point requires more heat loss to the atmosphere in autumn. In the marginal ice zone, the cooling and freezing process is mediated by ocean mixing and by the presence of remnant sea ice, which may precondition the ocean surface for refreezing. The delay in refreezing has many impacts, including increased open ocean exposure to autumn storms, additional wave energy incident to Arctic coasts, shifts in animal migration patterns, and extension of the time window for transit by commercial ships along the Northern Sea Route. This article reviews the observed trends in the western Arctic and the processes responsible for these trends, and provides brief in situ observations from the Beaufort Sea that illustrate some of these processes.

INTRODUCTION

The dramatic decline in Arctic sea ice cover over the past several decades is one of the most striking impacts of our warming climate and goes hand-in-hand with substantial changes in the length and timing of the summer melt season. Sea ice has tended to melt earlier in summer and re-form later in autumn (Stroeve et al., 2014; Stroeve and Notz, 2018). As we approach the time when an ice-free Arctic summer is expected, the fraction of the ice pack undergoing autumn freeze-up is increasing (Druckenmiller et al., 2021). While just over 50% of the ice pack was seasonal ice in 1980, over 70% of the ice pack has been seasonal in recent years (when defined as the difference between the minimum and maximum extent, relative to the maximum ice extent; see Figure 1). Once the Arctic has an ice-free summer, 100% of the ice will be seasonal. This is likely by 2070 even under a moderate emissions scenario (Jahn et al., 2016), and earlier under a higher-emissions scenario (Docquier and Koenigk, 2021); an assessment based on the observational record predicts it will occur by 2050 (Stroeve and Notz, 2018).

This article focuses on the freeze-up that occurs each autumn, along with its spring and summer preconditions (Steele et al., 2015). The freeze-up process includes complex air-ice-ocean feedback mechanisms at multiple scales that make it difficult to accurately predict future Arctic scenarios (e.g., Wang and Overland, 2015). Out of these complexities, one simple rule is clear: sea surface temperatures (SSTs) must cool to the freezing point before sea ice can form. The paper thus begins with an overview of pan-Arctic trends in sea ice and sea surface temperatures from satellite data, and then explores processes specific to the western Arctic, where substantial changes have motivated recent in situ observations. Following the western Arctic focus, the remaining sections of the paper discuss the broader impacts of delayed freeze-up and identify key topics for future research.

Sea Ice Trends

The open water season is lengthening, with freeze-up occurring later in the autumn (Stroeve et al., 2014). From 1979 to 2010, the timing of ice advance as observed by satellite was delayed more than one month (Stammerjohn et al., 2012). There is high correlation ($R^2 \approx 0.8$) between earlier sea ice retreat (and hence greater ocean heat uptake during summer) and later sea ice advance. The timing varies based on the threshold of sea ice cover used to consider the ocean ice-covered. Peng et al. (2018) report a trend in the freeze-up, where sea ice crosses 80% concentration, that is stronger than the trend in sea ice onset, where sea ice crosses 15% concentration. The average freeze-up shift in that study is 6.5 days later each decade, computed over 1979 to 2017. In Figure 2c, we plot the linear trend of the Arctic freeze-up date, defined as the date when the NOAA/NSIDC Climate Data Record of Passive Microwave Sea Ice Concentration (Meier et al., 2021) exceeds 80%. Trends are only calculated for cells in which there are at least 10 valid freeze-up dates over the record (i.e., sea ice concentration must go below 80% during the summer and above 80% during the winter). Models can allow us to explore different definitions of freeze-up beyond sea ice concentration, such as SST, sea ice volume changes, and rates of congelation or frazil ice growth. The trend in delay is clear and significant regardless of what metric is chosen (Smith and Jahn, 2019), underscoring the robustness of the signal.

Freeze onset dates are likely to continue to shift later. Under the high-emissions RCP8.5 future scenario, the Community Earth System Model (CESM) global climate model large ensemble suggests that the delay will more than double by the end of the twenty-first century (Smith and Jahn, 2019). This suggests an additional 2.5-month delay in average
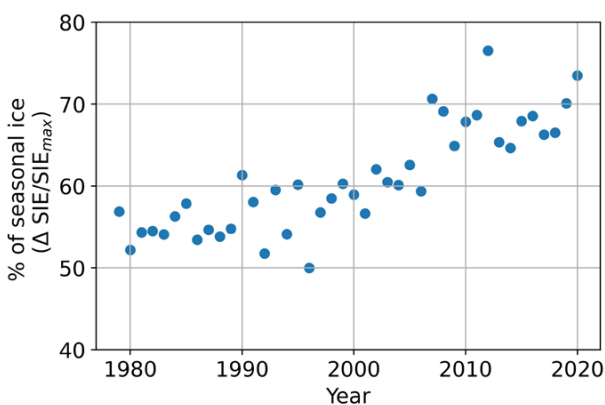

FIGURE 1. Percentage of Arctic sea ice extent (SIE) that is seasonal ice, defined as the difference between the minimum and maximum extent scaled by the maximum extent ($\Delta \text{SIE}/\text{SIE}_{max}$), over the satellite record. Data from the National Snow and Ice Data Center (NSIDC) via https://doi.org/10.7265/N5GT5K3K.

pan-Arctic freeze onset by 2099 is possible. Though model predictions are dramatic, the actual delay may be even more severe, given the historical under-prediction of sea ice loss by climate models (Notz and Stroeve, 2016). As discussed below, observed and future changes in the timing of Arctic sea ice freeze-up are mostly a forced response to atmospheric and ocean warming, but feedbacks such as preconditioning due to early melt onset and local ocean-ice-atmosphere interactions likely also play a role.

Figure 2 shows substantial regional variability in the magnitude of the delay. Due to the geometry of the Arctic Ocean, the trends for delay in ice advance are even stronger in coastal zones of a particular area (Onarheim et al., 2018).

For instance, in the Beaufort-Chukchi region, the ice advance along the coast portion has trended 1.2 days later per year through 2014, compared to 0.4 days later per year over the entire domain (Thomson et al., 2016).

Model studies show that the trend in freeze onset defined thermodynamically is stronger in open water areas than in those that remain partially ice covered (Smith and Jahn, 2019), suggesting the importance of feedbacks from solar ocean warming in driving these trends (Stammerjohn et al., 2012). In many coastal and fast ice regions, freeze-up timing is well predicted by melt onset timing, suggesting primarily thermodynamic factors (Stroeve et al., 2016). Freeze-up timing is also affected by

mechanical dynamics, and thus storms make freeze-up progression less predictable (Polyakov et al., 2022).

Sea Surface Temperature Trends

Figure 3a–c shows increased sea surface temperatures (SSTs) across most of the Arctic, which have been widely reported (Steele et al., 2008) and that are clearly related to changes in solar absorption (Steele et al., 2010). While SST is a useful metric for tracking oceanic changes, it is important to note that SST does not necessarily represent the heat content of the upper ocean, which is far more important to the freeze-up process. Open-water summer SSTs averaged over 2010–2019 are 1°–2°C warmer at the seasonal maxima than they were in the 1980s, with

(a) Date of Freeze-Up 1979–1988

(b) Date of Freeze-Up 2011–2020
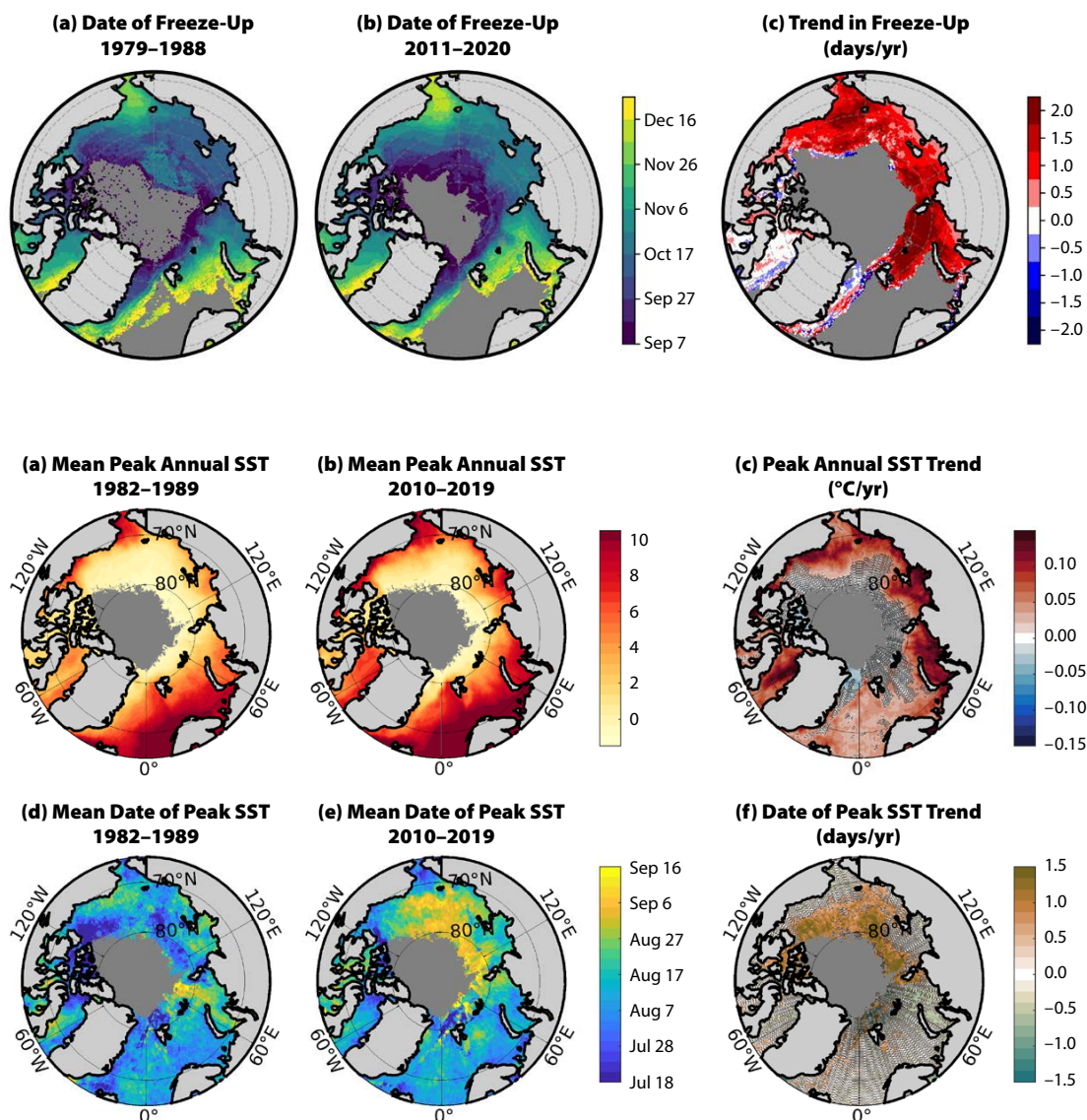
(c) Trend in Freeze-Up (days/yr)

FIGURE 2. Date of sea ice freeze-up (a) averaged over 1979–1988 and (b) 2011–2020, and (c) the trend (days/yr) over 1979–2020. Freeze-up is defined as when sea ice concentration from the NOAA/NSIDC Climate Data Record of Passive Microwave Sea Ice Concentration (Meier et al., 2021) exceeds 80%.

(a) Mean Peak Annual SST 1982–1989

(b) Mean Peak Annual SST 2010–2019

(c) Peak Annual SST Trend (°C/yr)

(d) Mean Date of Peak SST 1982–1989

(e) Mean Date of Peak SST 2010–2019

(f) Date of Peak SST Trend (days/yr)

FIGURE 3. (top) peak annual sea surface temperature (SST) averaged over (a) 1982–1989 and (b) 2010–2019, and (c) the trend over the 1982–2020 time period. (bottom) Date of peak annual SST averaged over (d) 1982–1989 and (e) 2010–2019, and (f) the trend over the 1982–2020 time period. Data are from the NOAA High-resolution Blended Analysis of Daily SST (OISST) 0.25° product from 1982 to 2020. SST data with sea ice concentration (from the NOAA/NSIDC product) greater than 80% are masked prior to processing. Grid points for which fewer than 75% of years have sufficient ice-free data to compute a trend are masked in dark gray, and those for which trend is not significant at the 95% level are stippled.

the greatest changes seen south of 75°N. A widespread warming trend exceeding 0.1°C yr⁻¹ is seen outside of the central Arctic Ocean and eastern Beaufort Sea (Figure 3c). In addition to warming, the timing of the annual peak SST (Figure 3d–f) has shifted significantly later in the year throughout much of the western Arctic. The warmest SSTs now occur in late August or early September, in comparison to the 1980s when SSTs peaked in late July (Figure 3d–f). In the Kara and Barents Seas, trends in annual peak SST are generally not significant. There are slight negative trends near the ice edge, which are an artifact of spatial averaging. The overall signal is an Arctic that is warmer in the autumn, with less and later sea ice as a direct result.

FREEZE-UP PROCESSES IN THE WESTERN ARCTIC

We now focus on the western Arctic and describe the dynamic and thermodynamic processes related to observed trends (Figure 4). In the western Arctic (Beaufort, Chukchi, and East Siberian Seas), trends in sea ice and SST are driven by inflow from the Pacific and by local heating; distinct water masses are important here (Nakanowatari et al., 2022). In the eastern Arctic marginal seas (e.g., Barents, Kara, and Laptev Seas), the key processes driving changes in SST and sea ice are quite different, including storm-driven upward transport of Atlantic Water heat and Atlantification, plus turbulent mixing above the continental slopes bordering Svalbard and Siberia. Eastern Arctic processes, which are beyond the scope of this paper, are discussed by Polyakov et al. (2017).

The cumulative decadal shifts in the western Arctic are illustrated by focusing on the month of October, the month that freeze-up has typically occurred and therefore the month in which long-term shifts in freeze-up are most clearly seen. Using the ERA5 reanalysis product, Figure 5 shows averages of October sea ice concentration, SST, and significant wave height from two decades:
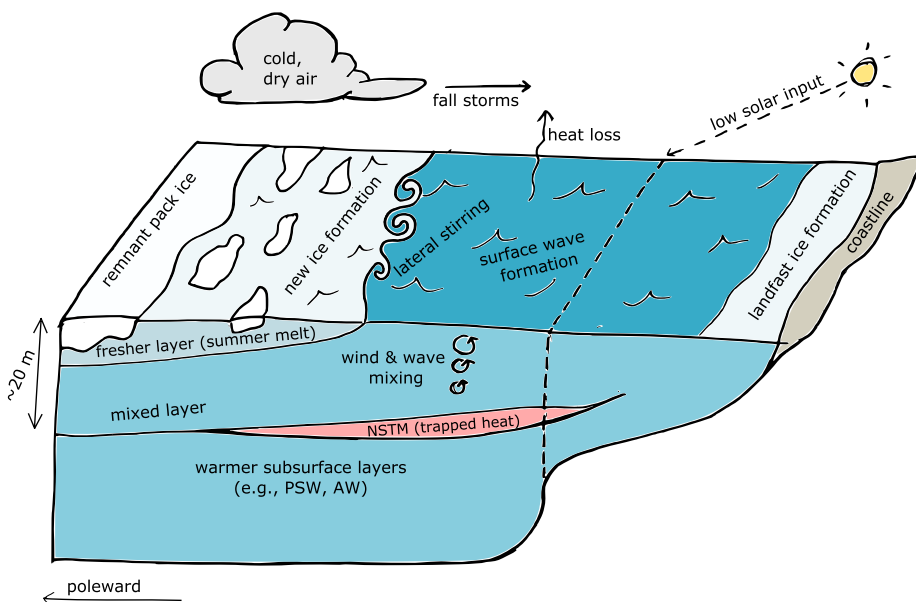

FIGURE 4. Schematic of key autumn freeze-up processes in the western Arctic. Storms generate wind and waves, driving heat flux out of the ocean that exceeds heat input from the sun, resulting in sea surface cooling and sea ice formation. Wind- and wave-generated mixing may also release heat trapped in the near-surface temperature maximum (NSTM), delaying freeze-up locally. In contrast, enhanced stratification from summer ice melt has the potential to sequester heat in the NSTM and hasten freeze-up.
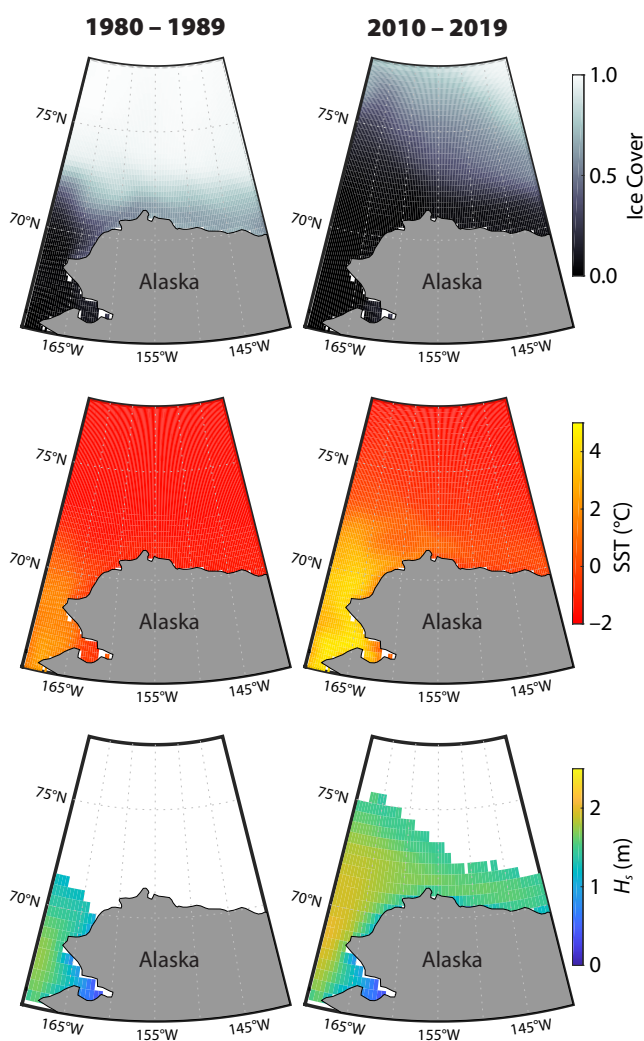

FIGURE 5. Average conditions for the month of October in the western Arctic from 1980–1989 (left) and 2010–2019 (right). Rows show sea ice concentration (top panel), sea surface temperature (SST, middle panel), and significant wave height (H_S, bottom panel) from the ERA5 reanalysis project, downloaded from https://cds.climate.copernicus.eu/.

1980–1989 and 2010–2019. The reduction in autumn ice cover is striking, as are the increases in SST and significant wave height. The relationship between SST and ice cover is thought to be both a cause and an effect, via the well-known ice-albedo feedback mechanism (Perovich et al., 2007). The increase in significant wave height is mostly a result of change in ice cover, which increases open-water fetch distances (Thomson and Rogers, 2014) and thereby increases wave heights, even in the absence of increasing winds (Thomson et al., 2016). Figure 5 suggests that the components of the air-ice-ocean system have combined to result in these seasonal shifts, each of which are explored in the following sections.

Heat Fluxes

Figure 4 shows the key processes in the autumn ice advance. The overall driver of ice formation is the loss of heat from the ocean to the atmosphere when large-scale atmospheric patterns bring cold air over warmer, open-water regions. As the input of solar heat decreases throughout the autumn, there are no external sources of heat to compensate for the loss to the atmosphere. There are, however, reservoirs of heat stored in the ocean. These reservoirs, discussed in more detail below, can reside below the surface because salinity controls stratification in most of the Arctic. Mixing controls the delivery of this stored heat to the ice-ocean interface, and thus its impact on ice formation. Upper ocean mixing is a complex interaction between processes that include direct forcing by surface winds and waves, lateral stirring by small-scale eddies and filaments, frontal dynamics, and internal ocean dynamics that generate vertical mixing, all of which are modulated by the strong near-surface stratification commonly found in this region (e.g., Brenner et al., 2020). As the freeze-up shifts later into the autumn, open water now coincides with stormier conditions and stronger upper ocean mixing (e.g., Smith et al., 2018).

Quantification of the processes in

Figure 4 typically applies a surface heat budget, in which the rate of change in heat at the ocean surface is expressed in fluxes:

$$Q_{net} = Q_{sw} + Q_{lw} + Q_{sensible} + Q_{latent} + Q_{sub}. \quad (1)$$

Positive values represent heat gain by the ocean and negative values represent heat loss. In the autumn, the input (gain) from the net shortwave radiative term, Q_{sw}, diminishes, and the overall net, Q_{net}, generally becomes negative (loss). The longwave radiative term, Q_{lw}, is itself a net term that can change sign depending on cloud conditions and sea surface temperature. The rate of sensible heat lost to the atmosphere, $Q_{sensible}$, is controlled by the air-water temperature difference. The rate of latent heat lost to the atmosphere, Q_{latent}, is also a function of the temperature difference, along with the relative humidity of the air. Cold and dry air masses originating over the perennial ice pack are thus excellent sinks of heat when they pass over open water. The sensible and latent terms also depend strongly on wind stress, and estimation of these terms is thus further complicated by uncertainties in the atmospheric drag coefficient in partial ice cover (Andreas et al., 2010; Persson et al., 2018). A heuristic final term represents a rate of subsurface ocean heat (mostly from the near-surface temperature maximum, or NSTM; see later section on Upper Ocean Heat) mixing up to the surface, Q_{sub}, which represents a heat gain to the surface but a heat loss from the NSTM.

The flux terms in the surface heat budget (Equation 1) are typically calculated from observations using the COARE (Coupled Ocean-Atmosphere Response Experiment) algorithm; see Fairall et al., 1996, 2003). This algorithm uses bulk average observations to estimate terms that are primarily turbulence driven, such as $Q_{sensible}$ and Q_{latent}, and thus are rarely measured directly. Obtaining accurate estimates of these terms (and thus Q_{net}) in the Arctic remains a key challenge for both observational and modeling efforts.

The total net rate Q_{net} controls how fast

the ocean surface cools in autumn, and, upon reaching a seawater freezing temperature of approximately −1.8°C, the rate of ice growth. The delay of autumn freeze-up is likely driven by a combination of adjustments to $Q_{sensible}$ and Q_{latent}, along with increases in Q_{sub}. The delay is also related to the simple truth that warmer initial sea surface temperatures must lose more heat (i.e., more sustained $Q_{net} < 0$) before reaching freezing temperature.

Atmospheric Forcing

Weather patterns are essential to autumn sea ice formation, especially in the western Arctic. Cold, dry air originating over sea ice can cause enormous sensible and latent heat loss from nearby open water regions (Persson et al., 2018). Thus, new ice growth is typically adjacent to the ice pack, and the progradation of the marginal ice zone is one common version of autumn freeze-up. Localized feedback mechanisms, such as low-level atmospheric jets that form along the ice edge (Guest et al., 2018), increase sensible and latent heat fluxes and potentially enhance vertical mixing.

Arctic air temperatures are increasing at rates about twice that of global warming (e.g., Serreze et al., 2009; Bekryaev et al., 2010; Dai et al., 2019). The effect on heat fluxes is significant. In areas with newly open water, there is much greater exchange between the ocean and the atmosphere (because the air-water temperature differences are larger). In areas that already had open water, the sensible heat losses are reduced. More specifically, the Arctic amplification observed in the warming trend is strongest in autumn and winter (Serreze and Barry, 2011; Dai et al., 2019). The reduction in cold air in autumn and the reduced rates of heat loss from the open ocean to the atmosphere are clear drivers for the delay of autumn freeze-up.

Atmospheric forcing also indirectly affects autumn freeze-up. Patterns in surface winds drive ocean circulation, which in turn affect the distribution of ocean temperatures. This can be particularly

important at regional scales. For example, an episodic shift in atmospheric circulation over the Bering Sea in 2018 increased the transport of warm water into the Chukchi Sea and delayed freeze-up that year (Kodaira et al., 2020). Wind-driven advection of sea ice also affects patterns of melt and freeze-up. Both these indirect and the direct mechanisms connect climate-scale atmospheric patterns to seasonal ice extent (Cai et al., 2021).

Autumn weather in the western Arctic is quite active, with cyclones forming and passing regularly through the region (Pichugin et al., 2019). Several studies have suggested that Arctic cyclones cause sea ice retreat in summer/autumn, as in the Great Arctic Cyclone of 2012 (Simmonds and Keay, 2012). However, recent work shows more nuanced effects, in which Arctic cyclones decrease ice in the eastern sector of the storm (where the air is warm and moist) and increase it in the storm's western sector (where the air is cold and dry; Clancy et al., 2021). The same work argues for equal importance of dynamic (i.e., motion) and thermodynamic (i.e., heat) effects on sea ice from Arctic cyclones. Looking to the future, there are clear linkages between the loss of ice and the large-scale atmospheric patterns (Moore et al., 2018; Ballinger et al., 2021; Valkonen et al., 2021). We can thus expect the atmosphere to continue to enhance delays in autumn freeze-up.

Upper Ocean Heat

Upper ocean heat content and the processes that deliver heat to the ice-ocean boundary layer modulate the timing and location of sea ice formation. Autumn freeze-up proceeds as waning shortwave radiation and colder air temperatures drive increased heat flux from the ocean surface layer into the atmosphere. During summer, solar input ($Q_{sw} + Q_{lw}$) is the dominant source of heat to the upper ocean (e.g., Maykut, 1982; Maykut and McPhee, 1995; Shaw et al., 2009). Once the solar input fades in autumn, cooling at the ocean surface is assured.

Strong surface layer freshening (McPhee et al., 1998; Solomon et al., 2021) has accompanied increased mixed layer temperatures in recent decades (Peralta-Ferriz and Woodgate, 2015), and is associated with changes in river runoff, precipitation, and sea ice melt or export (Haine et al., 2015). In the western Arctic, increasingly fresh inflow through the Bering Strait likely also plays a role (Woodgate and Peralta-Ferriz, 2021). At the cold temperatures (<5°C) typical of the Arctic upper ocean, seawater density is controlled primarily by salinity. Surface layer freshening thus strengthens the cold halocline, reinforcing the strong stratification that can isolate warmer waters below the mixed layer from the ice-ocean boundary layer above, enhancing surface cooling and promoting sea ice growth. This process can be patchy, with significant spatial variability (e.g., MacKinnon et al., 2021)

After the late-summer decrease in solar heat input each year, subsurface reservoirs of warm water, which are isolated from the ice-ocean boundary layer by the colder and fresher waters above, become the primary source of heat to the ice-ocean boundary layer. Atlantic waters that enter through Fram Strait and the Barents Sea circulate throughout the Arctic and represent the largest source of heat, though in the western Arctic these are too deep to provide much heat to the surface layer. The western Arctic typically exhibits two shallower, and thus more accessible, reservoirs of relatively warm waters. The shallowest, most accessible reservoir of heat is the NSTM (Jackson et al., 2010, 2011), which is typically found around 20 m to 30 m depth and is formed seasonally from surface waters that have been warmed by solar radiation and then capped by fresher, colder, more buoyant waters associated with sea ice melt (e.g., McPhee et al., 1998; Perovich et al., 2008). The NSTM provides short-term storage for summertime heating that is shallow enough to be released to the ice-ocean boundary layer by vertical mixing later in the autumn (e.g., Smith et al., 2018).

Pacific Summer Water (PSW) provides a second reservoir of heat in the western Arctic that is both larger and deeper (>40 m) than the NSTM. In summer, Pacific waters enter the Arctic through the Bering Strait (Woodgate, 2018), warming as they flow over the Chukchi Sea Shelf before they subduct below the fresher, more buoyant surface waters of the Beaufort Gyre (Timmermans et al., 2014). Subsurface eddies (Spall et al., 2008; Fine et al., 2018) and filaments (MacKinnon et al., 2021) inject these warm waters into the interior halocline. PSW is found throughout the Canada Basin (Timmermans et al., 2014) and has been associated with episodes of anomalous sea ice retreat over the Chukchi Sea and the southern Canada Basin (Shimada et al., 2006; Woodgate et al., 2010). Even in autumn, when cold air increases sensible heat loss, the PSW does not cool much before it subducts (and becomes isolated from the atmosphere). Thus, PSW is a source of heat to the region that arrives via a lateral process, but the effects of this heat are limited by vertical processes and may not have large basin-wide impacts on short (sub-seasonal) timescales. The PSW reservoir sits between 40 m and 100 m depth, within the cold halocline. Upper ocean stratification and diapycnal mixing exert strong control on the ability of PSW to supply heat to the ice-ocean boundary layer. In addition to the persistent water mass, pockets of anomalous PSW heat can persist for months to years within eddies moving through the region at the base of the mixed layer (Fine et al., 2018).

Lateral processes may also play an important role in the delivery and distribution of stored oceanic heat, especially along the marginal ice zone (MIZ; Manucharyan and Thompson, 2017). Energetic submesoscale turbulence can generate strong lateral stirring of heat and sea ice, as well as divergences with upwelling that can carry warm water to the surface locally. These are further enhanced by local winds and ice motion, which alter the otherwise persistent

lateral gradients (Brenner et al., 2020). These processes can drive rapid restratification (e.g., Boccaletti et al., 2007; Thomas et al., 2008; Timmermans et al., 2012) and likely modulate NSTM formation throughout summer and autumn. In some cases, fresh surface layers from ice melt may have sufficient stratification to inhibit mixing and thereby hasten sea ice formation by preconditioning the surface (Crews et al., 2022). This is an active area of research, with a large field campaign planned for autumn 2022 to sample stratification and surface fluxes near the autumn ice edge (https://salinity.oceansciences.org/sassie.htm).

Observations of an Autumn Ice Edge

In situ observations near the ice edge in the Beaufort Sea on September 30, 2020, illustrate many of the key processes that delay or accelerate ice formation during the initiation of freeze-up in the western Arctic. These observations are applied for estimating Q_{net} using the COARE algorithm and for demonstrating the

net balance that cools the ocean surface in autumn. The data presented here were collected opportunistically as part of a transit leg during the 2020 mooring recovery cruise for the Coastal Ocean Dynamics in the Arctic (CODA) program (http://www.apl.uw.edu/CODA). The observations span a marginal ice zone formed by remnant ice that had persisted in the southern Beaufort Sea for the entire summer of 2020. The overall minimum ice extent occurred on September 15, so these observations were made during the early stages of that year's large-scale freeze-up.

The observations were collected in an ice-following reference frame, spanning open water to nearly complete ice cover. Drifting buoys were used to establish the ice-following reference frame, which aids in diagnosing the evolution of temperature and salinity as purely temporal. Previous studies have used this approach to reduce the complications of interpreting changes that occur as ice advects through a spatial field (Smith et al., 2018; Brenner et al., 2020). Here,

four Surface Wave Instrument Float with Tracking (SWIFT; see Thomson, 2012, for description of the platform) buoys were deployed to freely drift for one day, while R/V *Sikuliaq* followed the drift and collected temperature and salinity profiles. Figure 6 shows the region of the sampling, along with an image of a SWIFT drifter in the ice. The practical salinity scale is used throughout (IOC, SCOR, and IAPSO, 2010).

The right panels of Figure 6 show the average salinity and temperature profiles collected in the ice and in open water, along with surface values from the SWIFTs. Although only separated by 6 km, the profiles in Figure 6 are notably different and demonstrate the preconditioning that influences freeze-up timing. As is typical for the MIZ, the surface waters in the ice are cold and fresh, relative to open water. However, even in broken ice, the SST is well above the nominal seawater freezing point of 1.8°C. Thus, heat loss Q_{net} must continue to occur before the MIZ refreezes into solid ice cover. The broken ice here is still melting, albeit slowly, until the freezing temperature is reached. The subsurface waters are the more notable part of this data set. The profile in open water has a strong NSTM around 10 m, relative to the weaker signal for the profile in the ice. It is expected that this NSTM resulted from the solar heating accumulated throughout the summer followed by surface cooling in the early autumn and possibly advected meltwater. Within the ice, the NSTM is thinner, weaker, and shallower because the higher albedo of partial ice cover has minimized the accumulation of solar heating during the summer.

The NSTM in open water is a reservoir of heat that can be released by ocean mixing (becoming Q_{sub}) to create large changes in Q_{net} that can delay the freeze-up by days and even weeks. Given the same atmospheric forcing, the area of broken ice is likely to refreeze much faster than the open water 6 km away. This would be true even without the difference in the surface temperatures, because
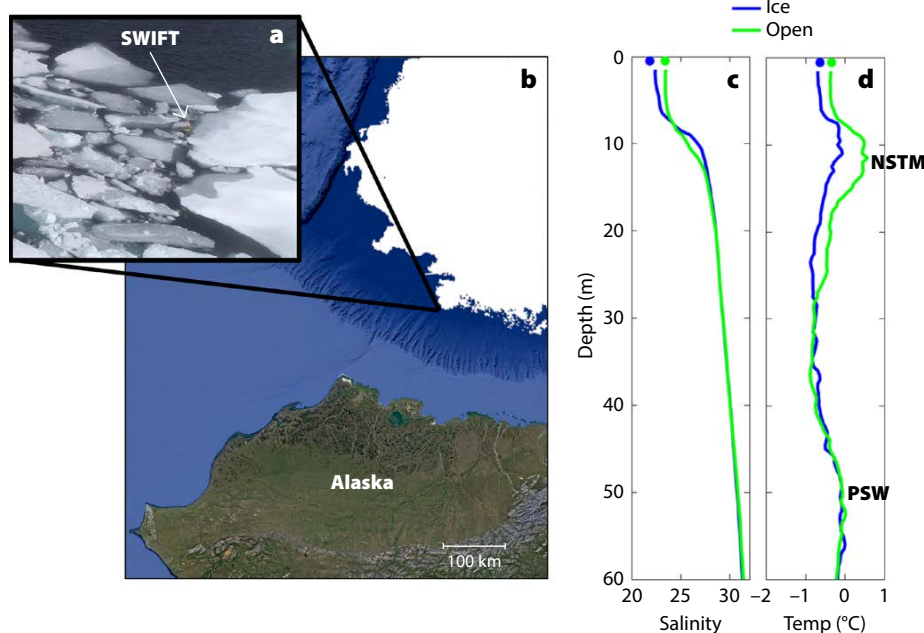

FIGURE 6. Data collection in the marginal ice zone of the Beaufort Sea on September 30, 2020. (a) Aerial image of the ice edge, in which a SWIFT drifter was sampling. *Image credit: Alex de Klerk* (b) Map showing ice cover (white) with sampling location. (c) Salinity profiles. (d) Temperature profiles. The surface points shown at the top of the profiles were measured by the SWIFT drifters, and the profiles were collected by shipboard CTD casting with a lateral separation of 6 km. PSW = Pacific Summer Water. NSTM = Near-surface temperature maximum. Ice cover from NSIDC via https://doi.org/10.7265/N5GT5K3K.

the total integrated heat of the NSTM will provide a Q_{sub} that controls Q_{net} in open water. Applying a seawater heat capacity of 3,850 J kg^{-1} C^{-1} to the temperature profiles in Figure 6, the open water profile has 4.2×10^7 J m^{-2} more heat than the profile in the ice. It would take 4.4 days of continuous heat loss at $Q_{net} = -100$ W m^{-2} for the open water profile to arrive at the same heat content as the profile in the ice (assuming no change in the ice profile). Lacking observations of the evolution of these profiles, we can only speculate that the actual heat loss is much more complicated, as Q_{net} varies over both profiles and some difference between them persists for weeks or more.

The speculated evolution toward freezing in this example becomes more quantitative upon estimating the heat fluxes (Equation 1) on the day the profiles were collected. Using the COARE algorithm (Fairall et al., 1996, 2003), the primary inputs are: air and water temperatures, relative humidity, wind speed, and radiation. The observed air temperature (−2°C) is always lower than the water temperature, leading to a steady loss of heat at the surface that is large in open water due to the stronger air-sea temperature gradient ($Q_{sensible} \sim -50$ Wm^{-2}). During daylight hours, the peak incoming shortwave radiation (Q_{sw} up to +150 W m^{-2}) exceeds this sensible heat loss and there is a brief net gain of heat in open water. The brief positive daytime surface flux is the lingering signal of the summer heating that originally formed the NSTM. This only occurs over open water; the albedo over the broken ice is much higher, and the net flux remains negative there. This brief example is representative of the early autumn ice edge, where spatial gradients modulate the heat fluxes as water temperatures evolve toward the freezing point. Recent work of Crews et al. (2022) uses autonomous systems to observe the full evolution of a similar region and provides a more comprehensive example.

Finally, we note the presence of PSW as secondary temperature maxima around 50 m in both profiles. As this is the result of inflow from Bering Strait, it is much more uniform across the region and does not have the kilometer-scale variation of the NSTM at the ice edge. Although the PSW does have a significant amount of total heat, it is generally too deep to mix up to the surface and affect Q_{net} on subseasonal timescales.

DISCUSSION

Feedbacks and Coupled Processes

Estimation of the heat fluxes that determine cooling and freeze-up is challenging. The COARE algorithm used to estimate fluxes in the prior section was originally developed for the tropics and has only sparse verification in the Arctic (Persson et al., 2018). The algorithm lacks explicit treatment of polar processes, such as heat loss from freezing spray (Blackmore and Lozowski, 1993) and changes to the atmospheric drag coefficient based on ice cover (Andreas et al., 2010). These processes need to be understood well enough that they can be formulated in robust parameterizations and then applied in predictive models.

The unsteady and heterogeneous nature of these coupled processes makes parameterization particularly challenging. The atmospheric drag coefficient that controls the flux of momentum from the atmosphere to the ocean (and/or sea ice) is sensitive to the stability of the lower atmosphere, which can change rapidly near the ice edge (Guest et al., 2018). Similarly, the ice drag coefficient that controls the flux of momentum from sea ice to the ocean below is sensitive to ice fraction and geometry (Tsamados et al., 2014; Brenner et al., 2021). Changes to momentum flux affect mixing and, thereby, fluxes of heat.

As discussed, prior melting in the marginal ice zone has a stabilizing effect, via salinity stratification, that can trap heat in the NSTM. Whether this heat can be mixed to the surface (and thus adjust Q_{net}) depends on the momentum flux through the stratified surface layer. Models require accurate drag coefficients to predict this process, and those drag coefficients evolve as well (i.e., depend on ice concentration, wind speed, atmospheric stability). Coupling air-ice-ocean models is becoming routine (Bromwich et al., 2018), but the uncertainty related to momentum and heat flux coefficients remains significant (Martin et al., 2016).

Surface waves have not been traditionally considered a key part of the coupled Arctic air-ice-ocean system, but surface wave activity in the Arctic is increasing (Wang et al., 2015; Stopa et al., 2016; Thomson et al., 2016) as a direct result of sea ice reduction (Thomson and Rogers, 2014). Not only are the open water fetch distances greater, but it is now more likely for open water to persist well into the autumn, when storms increase in frequency and severity. Even in partial ice cover, wave growth is a function of fetch and is increasing (Smith and Thomson, 2016; Gemmrich et al., 2018). The possible feedbacks between the waves and the ice are numerous, and the large-scale implications remain an active area of research.

Recent modeling efforts include two-way coupling of wave-ice evolution (Williams et al., 2017), in which waves can alter the prognostic floe size distribution of sea ice and sea ice attenuates waves across the whole Arctic (Roach et al., 2019). Such mechanisms would tend to exacerbate ice loss by providing more lateral melting of broken floes. Other processes, such as enhanced upward mixing of ocean heat caused by Langmuir turbulence, have also been shown to cause ice loss (Smith et al., 2018). Conversely, waves can enhance ice growth in the formation of pancake ice (Roach et al., 2018), which has become a more prevalent ice type in the Arctic in recent years (Thomson et al., 2018; Nose et al., 2020).

Impacts of Delayed Freeze-up

The dramatic delay in the autumn return of sea ice across the Arctic has numerous impacts beyond purely geophysical processes. Changes to Arctic coastal environments, to ecosystems, and to human use patterns provide a few examples.

One of the most notable impacts of more open water in the autumn is an increased wave climate. Figure 7 uses the ERA5 reanalysis product to demonstrate the increase in wave activity across the western Arctic. For the domain shown in Figure 5, the sum of the wave energy throughout the month of October is increasing. There is also significant inter-annual variability, including the remarkable persistence of open water in 1998 (Maslanik et al., 1999). The overall signal is a transition from an October that was nearly devoid of waves in the 1980s to one that is now very active. It is clear that this is a consequence of the delay in autumn freeze-up, which a few decades ago was nearly complete by the beginning of October (Figure 5).

The systematic delay of the autumn freeze-up means that Arctic coasts are exposed to more open ocean storms, which cause erosion and flooding (Overeem et al., 2011). The risk to permafrost coast-lines is particularly severe, with Alaskan coastlines identified as highly vulnerable and already manifesting shoreline retreat rates of several meters per year (Irrgang et al., 2022). The pan-Arctic shoreline loss is 0.5 m yr^{-1} (Lantuit et al., 2012), and the northern Alaska rate is 1.4 m yr^{-1} (Gibbs et al., 2015, 2019). The presence of land-fast ice does provide protection for the coasts (specifically from wave-driven pro-cesses), but that protection is preferen-tially in the spring (Hŏseková et al., 2021). In the autumn, newly forming ice along the coast is generally less effective in pro-tecting the coast from wave-driven pro-cesses (Hŏseková et al., 2020).

Rolph et al. (2018) examine the freeze-up trends of three Alaskan Arctic coastal communities and find delays of approximately one month in the date of freeze-up for communities exposed to the open ocean. Additionally, there has been an increase in the number of "false freeze-up" events, which suggests an increase in the length of time during which communities are left without reli-able ocean transport, as the ocean is neither suitable for boating nor frozen enough for on-ice travel. Various studies indicate that this problem will increase in the coming years (e.g., Casas-Prat and Wang, 2020).

In addition to changes in subsistence hunting and harvesting near the coasts, there are changes to human use pat-terns farther offshore. Interest in north-ern sea routes for commercial shipping has increased in recent years (Showstack, 2013), as have security concerns (US Navy, 2014, 2019). Already, there are estimates of conditions for commercial shipping in an ice-free Arctic (Nose et al., 2018). It is reasonable to expect that there will be more ship traffic as a direct conse-quence of a longer open-water season and less ice overall.

There are also changes to the Arctic ecosystem associated with delays in autumn freeze-up, including the north-ward shift of habitats and delays in migration (Baker et al., 2020). For exam-ple, recent work shows that polar cod, an essential part of the Arctic food web, are preferentially found beneath newly form-ing sea ice in autumn (Flores et al., 2020). Later ice thus means later polar cod, as well as the possibility of late autumn phytoplankton blooms (Ardyna et al., 2014). The long-term fate of larger ani-mals, such as polar bears, is also clearly tied to sea ice trends (Regehr et al., 2016). For the Indigenous communities with ongoing subsistence practices, these eco-system impacts are human impacts too. See Huntington et al. (2022) for a more complete description of the changes and challenges faced by local communities.

CONCLUSIONS

The autumn ice advance in the Arctic is happening later and later in the year, as part of a larger shift in the annual cycle of a warming planet. The trend is clear, even though many aspects of the relevant pro-cesses are still to be revealed. The seasonal ice advance is not a linear march south-ward as solar radiation declines. Rather, it is the evolution of a system controlled by atmospheric forcing, ocean memory, and multiple feedback mechanisms on both local and larger scales.

For the western Arctic Ocean (Canada Basin), the present state of knowledge about processes affecting delayed autumn freeze-up can be summarized as follows:

- There is an increased accumulation of ocean heat during summer months as a result of warming air temperatures and solar radiation.
- Ocean mixing events (i.e., storms) release subsurface heat in the autumn and thereby delay freeze-up.
- Strong lateral gradients and instabil-ities present at the evolving ice edge modulate the mixing events.
- The ocean can be preconditioned to refreeze by the presence of remnant sea ice.
- There is strong coupling at the atmo-sphere-ocean-ice boundary, including possible feedback mechanisms related to surface wave action.

It is highly certain that the delay in freeze-up will continue and grow, yet there is more work to be done in under-standing the coupled processes that drive both freeze-up and its delay. To advance the state of knowledge, and to improve model predictive skill, we identify several needs for future work, including:

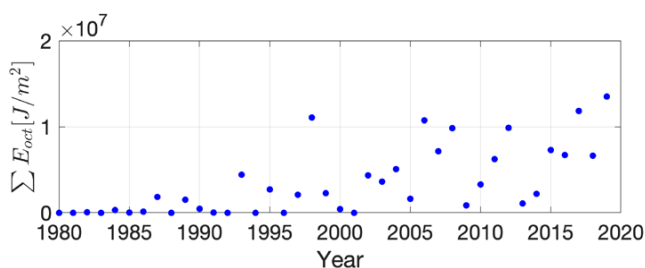- Understand the drivers and impacts of near-surface (0–5 m) stratification during freeze-up.

FIGURE 7. Cumulative wave energy in the western Arctic (region defined in Figure 5) from each October 1979–2020, based on ERA5 reanal-ysis data.

- Determine the importance of lateral shear and associated mixing near the evolving ice edge.
- Develop a polar-specific version of the COARE algorithm to estimate bulk air-sea fluxes in the presence of sea ice, including improved parameterizations (e.g., drag coefficients) for air-sea exchanges of heat and momentum rather than coupling.
- Refine fully coupled atmosphere-ocean-ice models that include possible feedback mechanisms with surface wave activity.

Addressing these needs will require distributed observations of autumn freeze-up across the Arctic, especially sustained observations at or near the ocean surface. Autonomous platforms offer a promising approach to collecting data near the surface interface with minimal disturbances, but they present challenges in endurance and navigation (Meinig et al., 2015; Lee and Thomson, 2017; Zhang et al., 2019; Grare et al., 2021). Despite numerous recent and ongoing field efforts, there remains a gap in the observations needed to calibrate and validate heat flux estimates. These recommendations seek both to improve the accuracy of predictive models and to improve fundamental understanding of the Arctic system. ⊚

REFERENCES

Andreas, E.L., P.O.G. Persson, A.A. Grachev, R.E. Jordan, T.W. Horst, P.S. Guest, and C.W. Fairall. 2010. Parameterizing turbulent exchange over sea ice in winter. *Journal of Hydrometeorology* 11(1):87–104, https://doi.org/10.1175/2009JHM1102.1.

Ardyna, M., M. Babin, M. Gosselin, E. Devred, L. Rainville, and J.-E. Tremblay. 2014. Recent Arctic Ocean sea ice loss triggers novel fall phytoplankton blooms. *Geophysical Research Letters* 41(17):6,207–6,212, https://doi.org/10.1002/2014GL061047.

Baker, M.R., E.V. Farley, C. Ladd, S.L. Danielson, K.M. Stafford, H.P. Huntington, and D.M. Dickson. 2020. Integrated ecosystem research in the Pacific Arctic − Understanding ecosystem processes, timing and change. *Deep Sea Research Part II* 177:104850, https://doi.org/10.1016/j.dsr2.2020.104850.

Ballinger, T.J., J.E. Walsh, U.S. Bhatt, P.A. Bieniek, M.A. Tschudi, B. Brettschneider, H. Eicken, A.R. Mahoney, J. Richter-Menge, and L.H. Shapiro. 2021. Unusual west Arctic storm activity during winter 2020: Another collapse of the Beaufort high? *Geophysical Research Letters* 48(13), https://doi.org/10.1029/2021GL092518.

Bekryaev, R.V., I.V. Polyakov, and V.A. Alexeev. 2010. Role of polar amplification in long-term surface air temperature variations and modern Arctic warming. *Journal of Climate* 23(14):3,888–3,906, https://doi.org/10.1175/2010JCLI3297.1.

Blackmore, R., and E. Lozowski. 1993. An heuristic freezing spray model of vessel icing. *International Ocean and Polar Engineering Conference*, ISOPE-I-93-196.

Boccaletti, G., R. Ferrari, and B. Fox-Kemper. 2007. Mixed layer instabilities and restratification. *Journal of Physical Oceanography* 37(9):2,228–2,250, https://doi.org/10.1175/JPO3101.1.

Bromwich, D.H., A.B. Wilson, L. Bai, Z. Liu, M. Barlage, C.-F. Shih, S. Maldonado, K.M. Hines, S.-H. Wang, J. Woollen, and others. 2018. The Arctic system reanalysis, version 2. *Bulletin of the American Meteorological Society* 99(4):805–828, https://doi.org/10.1175/BAMS-D-16-0215.1.

Brenner, S., L. Rainville, J. Thomson, and C. Lee. 2020. The evolution of a shallow front in the Arctic marginal ice zone. *Elementa: Science of the Anthropocene* 8(1):17, https://doi.org/10.1525/elementa.413.

Brenner, S., L. Rainville, J. Thomson, S. Cole, and C. Lee. 2021. Comparing observations and parameterizations of ice-ocean drag through an annual cycle across the Beaufort Sea. *Journal of Geophysical Research: Oceans* 126(4):e2020JC016977, https://doi.org/10.1029/2020JC016977.

Cai, Q., D. Beletsky, J. Wang, and R. Lei. 2021. Interannual and decadal variability of Arctic summer sea ice associated with atmospheric teleconnection patterns during 1850–2017. *Journal of Climate* 34(24):9,931–9,955, https://doi.org/10.1175/JCLI-D-20-0330.1.

Casas-Prat, M., and X.L. Wang. 2020. Projections of extreme ocean waves in the Arctic and potential implications for coastal inundation and erosion. *Journal of Geophysical Research: Oceans* 125(8):e2019JC015745, https://doi.org/10.1029/2019JC015745.

Clancy, R., C.M. Bitz, E. Blanchard-Wrigglesworth, M.C. McGraw, and S.M. Cavallo. 2021. A cyclone-centered perspective on the drivers of asymmetric patterns in the atmosphere and sea ice during Arctic cyclones. *Journal of Climate*, https://doi.org/10.1175/JCLI-D-21-0093.1.

Crews, L., C.M. Lee, L. Rainville, and J. Thomson. 2022. Direct observations of the role of lateral advection of sea ice meltwater in the onset of autumn freeze up. *Journal of Geophysical Research: Oceans*, https://doi.org/10.1029/2021JC017775.

Dai, A., D. Luo, M. Song, and J. Liu. 2019. Arctic amplification is caused by sea-ice loss under increasing CO_2. *Nature Communications* 10(1):121, https://doi.org/10.1038/s41467-018-07954-9.

Docquier, D., and T. Koenigk. 2021. Observation-based selection of climate models projects Arctic ice-free summers around 2035. *Communications Earth & Environment* 2:144, https://doi.org/10.1038/s43247-021-00214-7.

Druckenmiller, M.L., T.A. Moon, R.L. Thoman, T.J. Ballinger, L.T. Berner, G.H. Bernhard, U.S. Bhatt, J.W. Bjerke, J.E. Box, R. Brown, and others. 2021. The Arctic. *Bulletin of the American Meteorological Society* 102(8):S263–S316, https://doi.org/10.1175/BAMS-D-21-0086.1.

Fairall, C.W., E.F. Bradley, D.P. Rogers, J.B. Edson, and G.S. Young. 1996. Bulk parameterization of air-sea fluxes for TOGA COARE. *Journal of Geophysical Research* 101:3,747–3,764, https://doi.org/10.1029/95JC03205.

Fairall, C., E. Bradley, J. Hare, A. Grachev, and J. Edson. 2003. Bulk parameterization of air-sea fluxes: Updates and verification for the COARE algorithm. *Journal of Climate* 16:571–591, https://doi.org/10.1175/1520-0442(2003)016<0571:BPOASF>2.0.CO;2.

Fine, E.C., J.A. MacKinnon, M.H. Alford, and J.B. Mickett. 2018. Microstructure observations of turbulent heat fluxes in a warm-core Canada Basin eddy. *Journal of Physical Oceanography* 48(10):2,397–2,418, https://doi.org/10.1175/JPO-D-18-0028.1.

Flores, H., F. Mueter, R. ten Boer, M. van Dorssen, L. Edenfield, A. Klasmeier, K. Kunz, S. Maes, A. Pinchuk, J. Weems, and N. Zakharova. 2020. Go West: Sea-ice association of polar cod and its prey in the western Arctic Ocean. Alfred Wegener Institut, R/V *Sikuliaq* Cruise No. SKQ201923S Report, https://epic.awi.de/id/eprint/51865/.

Gemmrich, J., W.E. Rogers, J. Thomson, and S. Lehner. 2018. Wave evolution in off-ice wind conditions. *Journal of Geophysical Research: Oceans* 123(12), https://doi.org/10.1029/2018JC013793.

Gibbs, A., K. Ohman, and B. Richmond. 2015. *National Assessment of Shoreline Change—A GIS Compilation of Vector Shorelines and Associated Shoreline Change Data for the North Coast of Alaska, U.S.-Canadian Border to Icy Cape*. Open-File Report 2015-1030, US Geological Survey, https://doi.org/10.3133/ofr20151030.

Gibbs, A.E., M. Nolan, B.M. Richmond, A.G. Snyder, and L.H. Erikson. 2019. Assessing patterns of annual change to permafrost bluffs along the north slope coast of Alaska using high-resolution imagery and elevation models. *Geomorphology* 336:152–164, https://doi.org/10.1016/j.geomorph.2019.03.029.

Grare, L., N.M. Statom, N. Pizzo, and L. Lenain. 2021. Instrumented wave gliders for air-sea interaction and upper ocean research. *Frontiers in Marine Science* 8:888, https://doi.org/10.3389/fmars.2021.664728.

Guest, P., P.O.G. Persson, S. Wang, M. Jordan, Y. Jin, B. Blomquist, and C. Fairall. 2018. Low-level baroclinic jets over the new Arctic Ocean. *Journal of Geophysical Research: Oceans* 123(6):4,074–4,091, https://doi.org/10.1002/2018JC013778.

Haine, T.W., B. Curry, R. Gerdes, E. Hansen, M. Karcher, C. Lee, B. Rudels, G. Spreen, L. de Steur, K.D. Stewart, and others. 2015. Arctic freshwater export: Status, mechanisms, and prospects. *Global and Planetary Change* 125:13–35, https://doi.org/10.1016/j.gloplacha.2014.11.013.

Hōseková, L., M.P. Malila, W.E. Rogers, L.A. Roach, E. Eidam, L. Rainville, N. Kumar, and J. Thomson. 2020. Attenuation of ocean surface waves in pancake and frazil sea ice along the coast of the Chukchi Sea. *Journal of Geophysical Research: Oceans* 125(12), https://doi.org/10.1029/2020JC016746.

Hōseková, L., E. Eidam, G. Panteleev, L. Rainville, W.E. Rogers, and J. Thomson. 2021. Landfast ice and coastal wave exposure in northern Alaska. *Geophysical Research Letters* 48(22):e2021GL095103, https://doi.org/10.1029/2021GL095103.

Huntington, H. P., A. Zagorsky, B.P. Kaltenborn, H.C. Shin, J. Dawson, M. Lukin, P.E. Dahl, P. Guo, and D.N. Thomas. 2022. Societal implications of a changing Arctic Ocean. *Ambio* 51(2):298–306, https://doi.org/10.1007/s13280-021-01601-2.

IOC, SCOR and IAPSO. 2010. *The International Thermodynamic Equation of Seawater—2010: Calculation and Use of Thermodynamic Properties*. Intergovernmental Oceanographic Commission, Manuals and Guides No. 56, UNESCO, 196 pp.

Irrgang, A.M., M. Bendixen, L.M. Farquharson, A.V. Baranskaya, L.H. Erikson, A.E. Gibbs, S.A. Ogorodov, P.P. Overduin, H. Lantuit, M.N. Grigoriev, and B.M. Jones. 2022. Drivers, dynamics and impacts of changing Arctic coasts. *Nature Reviews Earth & Environment* 3(1):39–54, https://doi.org/10.1038/s43017-021-00232-1.

Jackson, J.M., E.C. Carmack, F.A. McLaughlin, S.E. Allen, and R.G. Ingram. 2010. Identification, characterization, and change of the near-surface temperature maximum in the Canada Basin, 1993–2008. *Journal of Geophysical Research: Oceans* 115(C5), https://doi.org/10.1029/2009JC005265.

Jackson, J.M., S.E. Allen, F. McLaughlin, R. Woodgate, and E. Carmack. 2011. Changes to the near-surface waters in the Canada Basin, Arctic Ocean from 1993–2009: A basin in transition. *Journal of Geophysical Research: Oceans* 116(C10), https://doi.org/10.1029/2011JC007069.

Jahn, A., J.E. Kay, M.M. Holland, and D.M. Hall. 2016. How predictable is the timing of a summer ice-free Arctic? *Geophysical Research Letters* 43(17):9,113–9,120, https://doi.org/10.1002/2016GL070067.

Kodaira, T., T. Waseda, T. Nose, and J. Inoue. 2020. Record high Pacific Arctic seawater temperatures and delayed sea ice advance in response to episodic atmospheric blocking. *Scientific Reports* 10:20830, https://doi.org/10.1038/s41598-020-77488-y.

Lantuit, H., P.P. Overduin, N. Couture, S. Wetterich, F. Aré, D. Atkinson, J. Brown, G. Cherkashov, D. Drozdov, D.L. Forbes, and others. 2012. The Arctic coastal dynamics database: A new classification scheme and statistics on Arctic permafrost coastlines. *Estuaries and Coasts* 35(2):383–400, https://doi.org/10.1007/s12237-010-9362-6.

Lee, C., and J. Thomson. 2017. An autonomous approach to observing the seasonal ice zone. *Oceanography* 30(2):56–68, https://doi.org/10.5670/oceanog.2017.222.

MacKinnon, J.A., H.L. Simmons, J. Hargrove, J. Thomson, T. Peacock, M.H. Alford, B.I. Barton, S. Boury, S.D. Brenner, N. Couto, and others. 2021. A warm jet in a cold ocean. *Nature Communications* 12(1):2418, https://doi.org/10.1038/s41467-021-22505-5.

Manucharyan, G.E., and A.F. Thompson. 2017. Submesoscale sea ice-ocean interactions in marginal ice zones. *Journal of Geophysical Research: Oceans* 122(12):9,455–9,475, https://doi.org/10.1002/2017JC012895.

Martin, T., M. Tsamados, D. Schroeder, and D.L. Feltham. 2016. The impact of variable sea ice roughness on changes in Arctic Ocean surface stress: A model study. *Journal of Geophysical Research: Oceans* 121(3):1,931–1,952, https://doi.org/10.1002/2015JC011186.

Maslanik, J.A., M.C. Serreze, and T. Agnew. 1999. On the record reduction in 1998 western Arctic sea-ice cover. *Geophysical Research Letters* 26(13):1,905–1,908, https://doi.org/10.1029/1999GL900426.

Maykut, G.A. 1982. Large-scale heat exchange and ice production in the central Arctic. *Journal of Geophysical Research: Oceans* 87(C10):7,971–7,984, https://doi.org/10.1029/JC087iC10p07971.

Maykut, G., and M.G. McPhee. 1995. Solar heating of the Arctic mixed layer. *Journal of Geophysical Research: Oceans* 100(C12):24,691–24,703, https://doi.org/10.1029/95JC02554.

McPhee, M.G., T.P. Stanton, J.H. Morison, and D.G. Martinson. 1998. Freshening of the upper ocean in the Arctic: Is perennial sea ice disappearing? *Geophysical Research Letters* 25(10):1,729–1,732, https://doi.org/10.1029/98GL00933.

Meier, W.N., F. Fetterer, A.K. Windnagel, and J.S. Stewart. 2021. NOAA/NSIDC Climate Data Record of Passive Microwave Sea Ice Concentration, Version 4. National Snow and Ice Data Center, https://nsidc.org/data/G02202/versions/4.

Meinig, C., N. Lawrence-Slavas, R. Jenkins, and H.M. Tabisola. 2015. The use of Saildrones to examine spring conditions in the Bering Sea: Vehicle specification and mission performance. In *Proceedings of OCEANS 2015 - MTS/IEEE Washington*, conference held October 19–22, Washington, DC, https://doi.org/10.23919/OCEANS.2015.7404348.

Moore, G.W.K., A. Schweiger, J. Zhang, and M. Steele. 2018. Collapse of the 2017 winter Beaufort high: A response to thinning sea ice? *Geophysical Research Letters* 45(6):2,860–2,869, https://doi.org/10.1002/2017GL076446.

Nakanowatari, T., J. Inoue, J. Zhang, E. Watanabe, and H. Kuroda. 2022. A new norm for seasonal sea ice advance predictability in the Chukchi Sea: Rising influence of ocean heat advection. *Journal of Climate* 35(9):2,723–2,740, https://doi.org/10.1175/JCLI-D-21-0425.1.

Nose, T., A. Webb, T. Waseda, J. Inoue, and K. Sato. 2018. Predictability of storm wave heights in the ice-free Beaufort Sea. *Ocean Dynamics* 68(10):1,383–1,402, https://doi.org/10.1007/s10236-018-1194-0.

Nose, T., T. Waseda, T. Kodaira, and J. Inoue. 2020. On the coagulated pancake ice formation: Observation in the refreezing Chukchi Sea and comparison to the Antarctic consolidated pancake ice. *Polar Science* 27:100622, https://doi.org/10.1016/j.polar.2020.100622.

Notz, D., and J. Stroeve. 2016. Observed Arctic sea-ice loss directly follows anthropogenic CO_2 emission. *Science* 354(6313):747–750, https://doi.org/10.1126/science.aag2345.

Onarheim, I.H., T. Eldevik, L.H. Smedsrud, and J.C. Stroeve. 2018. Seasonal and regional manifestation of Arctic sea ice loss. *Journal of Climate* 31(12):4,917–4,932, https://doi.org/10.1175/JCLI-D-17-0427.1.

Overeem, I., R.S. Anderson, C.W. Wobus, G.D. Clow, F.E. Urban, and N. Matell. 2011. Sea ice loss enhances wave action at the Arctic coast. *Geophysical Research Letters* 38(17), https://doi.org/10.1029/2011GL048681.

Peng, G., M. Steele, A.C. Bliss, W.N. Meier, and S. Dickinson. 2018. Temporal means and variability of Arctic sea ice melt and freeze season climate indicators using a satellite climate data record. *Remote Sensing* 10(9):1328, https://doi.org/10.3390/rs10091328.

Peralta-Ferriz, C., and R.A. Woodgate. 2015. Seasonal and interannual variability of pan-Arctic surface mixed layer properties from 1979 to 2012 from hydrographic data, and the dominance of stratification for multiyear mixed layer depth shoaling. *Progress in Oceanography* 134:19–53, https://doi.org/10.1016/j.pocean.2014.12.005.

Perovich, D.K., B. Light, H. Eicken, K.F. Jones, K. Runciman, and S.V. Nghiem. 2007. Increasing solar heating of the Arctic Ocean and adjacent seas, 1979–2005: Attribution and role in the ice-albedo feedback. *Geophysical Research Letters* 34(19), https://doi.org/10.1029/2007GL031480.

Perovich, D.K., J.A. Richter-Menge, K.F. Jones, and B. Light. 2008. Sunlight, water, and ice: Extreme arctic sea ice melt during the summer of 2007. *Geophysical Research Letters* 35(11), https://doi.org/10.1029/2008GL034007.

Persson, O., B. Blomquist, P. Guest, S. Stammerjohn, C. Fairall, L. Rainville, B. Lund, S. Ackley, and J. Thomson. 2018. Shipboard observations of the meteorology and near-surface environment during autumn freezeup in the Beaufort/Chukchi Seas. *Journal of Geophysical Research: Oceans* 123(2):4,930–4,969, https://doi.org/10.1029/2018JC013786.

Pichugin, M.K., I.A. Gurvich, and E.V. Zabolotskikh. 2019. Severe marine weather systems during freeze-up in the Chukchi Sea: Cold-air outbreak and mesocyclone case studies from satellite multisensor measurements and reanalysis datasets. *IEEE Journal of Selected Topics in Applied Earth Observations and Remote Sensing* 12(9):3,208–3,218, https://doi.org/10.1109/JSTARS.2019.2934749.

Polyakov, I.V., A.V. Pnyushkov, M.B. Alkire, I.M. Ashik, T.M. Baumann, E.C. Carmack, I. Goszczko, J. Guthrie, V.V. Ivanov, T. Kanzow, and others. 2017. Greater role for Atlantic inflows on sea-ice loss in the Eurasian Basin of the Arctic Ocean. *Science* 356(6335):285–291, https://doi.org/10.1126/science.aai8204.

Polyakov, I.V., M. Mayer, S. Tietsche, and A.Y. Karpechko. 2022. Climate change fosters competing effects of dynamics and thermodynamics in seasonal predictability of Arctic sea ice. *Journal of Climate* 35(9):2,849–2,865, https://doi.org/10.1175/JCLI-D-21-0463.1.

Regehr, E.V., K.L. Laidre, H.R. Akçakaya, S.C. Amstrup, T.C. Atwood, N.J. Lunn, M. Obbard, H. Stern, G.W. Thiemann, and Ø. Wiig. 2016. Conservation status of polar bears (*Ursus maritimus*) in relation to projected sea-ice declines. *Biology Letters* 12(12):20160556, https://doi.org/10.1098/rsbl.2016.0556.

Roach, L.A., M.M. Smith, and S.M. Dean. 2018. Quantifying growth of pancake sea ice floes using images from drifting buoys. *Journal of Geophysical Research: Oceans* 123(12), https://doi.org/10.1002/2017JC013693.

Roach, L.A., C.M. Bitz, C. Horvat, and S.M. Dean. 2019. Advances in modeling interactions between sea ice and ocean surface waves. *Journal of Advances in Modeling Earth Systems* 11(12):4,167–4,181, https://doi.org/10.1029/2019MS001836.

Rolph, R.J., A.R. Mahoney, J. Walsh, and P.A. Loring. 2018. Impacts of a lengthening open water season on Alaskan coastal communities: Deriving locally relevant indices from large-scale datasets and community observations. *The Cryosphere* 12(5):1,779–1,790, https://doi.org/10.5194/tc-12-1779-2018.

Serreze, M., A. Barrett, J. Stroeve, D. Kindig, and M. Holland. 2009. The emergence of surface-based arctic amplification. *The Cryosphere* 3(1):11–19, https://doi.org/10.5194/tc-3-11-2009.

Serreze, M.C., and R.G. Barry. 2011. Processes and impacts of Arctic amplification: A research synthesis. *Global and Planetary Change* 77(1–2):85–96, https://doi.org/10.1016/j.gloplacha.2011.03.004.

Shaw, W., T. Stanton, M. McPhee, J. Morison, and D. Martinson. 2009. Role of the upper ocean in the energy budget of Arctic sea ice during SHEBA. *Journal of Geophysical Research: Oceans* 114(C6), https://doi.org/10.1029/2008JC004991.

Shimada, K., T. Kamoshida, M. Itoh, S. Nishino, E. Carmack, F. McLaughlin, S. Zimmermann, and A. Proshutinsky. 2006. Pacific Ocean inflow: Influence on catastrophic reduction of sea ice cover in the Arctic Ocean. *Geophysical Research Letters* 33(8), https://doi.org/10.1029/2005GL025624.

Showstack, R. 2013. Diminishing sea ice in the Arctic presents challenges and opportunities. *Eos, Transactions, American Geophysical Union* 94(31):270–271, https://doi.org/10.1002/2013EO310002.

Simmonds, I.K., and I. Rudeva. 2012. The great Arctic cyclone of August 2012. *Geophysical Research Letters* 39 (23), https://doi.org/10.1029/2012GL054259.

Smith, M., and J. Thomson. 2016. Scaling observations of surface waves in the Beaufort Sea. *Elementa: Science of the Anthropocene* 4:000097, https://doi.org/10.12952/journal.elementa.000097.

Smith, M., S. Stammerjohn, O. Persson, L. Rainville, G. Liu, W. Perrie, R. Robertson, J. Jackson, and J. Thomson. 2018. Episodic reversal of autumn ice advance caused by release of ocean heat in the Beaufort Sea. *Journal of Geophysical Research: Oceans* 123(5):3,164–3,185, https://doi.org/10.1002/2018JC013764.

Smith, A., and A. Jahn. 2019. Definition differences and internal variability affect the simulated Arctic sea ice melt season. *The Cryosphere* 13(1):1–20, https://doi.org/10.5194/tc-13-1-2019.

Solomon, A., C. Heuzé, B. Rabe, S. Bacon, L. Bertino, P. Heimbach, J. Inoue, D. Iovino, R. Mottram, X. Zhang, and others. 2021. Freshwater in the Arctic Ocean 2010–2019. *Ocean Science* 17(4):1,081–1,102, https://doi.org/10.5194/os-17-1081-2021.

Spall, M.A., R.S. Pickart, P.S. Fratantoni, and A.J. Plueddemann. 2008. Western Arctic shelf-break eddies: Formation and transport. *Journal of Physical Oceanography* 38(8):1,644–1,668, https://doi.org/10.1175/2007JPO3829.1.

Stammerjohn, S., R. Massom, D. Rind, and D. Martinson. 2012. Regions of rapid sea ice change: An inter-hemispheric seasonal comparison. *Geophysical Research Letters* 39(6), https://doi.org/10.1029/2012GL050874.

Steele, M., W. Ermold, and J. Zhang. 2008. Arctic Ocean surface warming trends over the past 100 years. *Geophysical Research Letters* 35(2), https://doi.org/10.1029/2007GL031651.

Steele, M., J. Zhang, and W. Ermold. 2010. Mechanisms of summertime upper Arctic Ocean warming and the effect on sea ice melt. *Journal of Geophysical Research: Oceans* 115(C11), https://doi.org/10.1029/2009JC005849.

Steele, M., S. Dickinson, J. Zhang, and R.W. Lindsay. 2015. Seasonal ice loss in the Beaufort Sea: Toward synchrony and prediction. *Journal of Geophysical Research: Oceans* 120(2):1,118–1,132, https://doi.org/10.1002/2014JC010247.

Stopa, J.E., F. Ardhuin, and F. Girard-Adrhuin. 2016. Wave-climate in the Arctic 1992–2014: Seasonality, trends, and wave-ice influence. *The Cryosphere* 10(4):1,605–1,629, https://doi.org/10.5194/tc-10-1605-2016.

Stroeve, J.C., T. Markus, L. Boisvert, J. Miller, and A. Barrett. 2014. Changes in Arctic melt season and implications for sea ice loss. *Geophysical Research Letters* 41(4):1,216–1,225, https://doi.org/10.1002/2013GL058951.

Stroeve, J.C., A.D. Crawford, and S. Stammerjohn. 2016. Using timing of ice retreat to predict timing of fall freeze-up in the Arctic. *Geophysical Research Letters* 43(12):6,332–6,340, https://doi.org/10.1002/2016GL069314.

Stroeve, J., and D. Notz. 2018. Changing state of Arctic sea ice across all seasons. *Environmental Research Letters* 13(10):103001, https://doi.org/10.1088/1748-9326/aade56.

Thomas, L.N., A. Tandon, and A. Mahadevan. 2008. Submesoscale processes and dynamics. Pp. 17–38 in *Ocean Modeling in an Eddying Regime,* vol. 177. AGU Geophysical Monograph Series, https://doi.org/10.1029/177GM04.

Thomson, J. 2012. Wave breaking dissipation observed with SWIFT drifters. *Journal of Atmospheric and Oceanic Technology* 29(12):1,866–1,882, https://doi.org/10.1175/JTECH-D-12-00018.1.

Thomson, J., and W.E. Rogers. 2014. Swell and sea in the emerging Arctic Ocean. *Geophysical Research Letters* 41(9):3,136–3,140, https://doi.org/10.1002/2014GL059983.

Thomson, J., Y. Fan, S. Stammerjohn, J. Stopa, W.E. Rogers, F. Girard-Ardhuin, F. Ardhuin, H. Shen, W. Perrie, H. Shen, and others. 2016. Emerging trends in the sea state of the Beaufort and Chukchi Seas. *Ocean Modelling* 105:1–12, https://doi.org/10.1016/j.ocemod.2016.02.009.

Thomson, J., S. Ackley, F. Girard-Ardhuin, F. Ardhuin, A. Babanin, G. Boutin, J. Brozena, S. Cheng, C. Collins, M. Doble, and others. 2018. Overview of the Arctic sea state and boundary layer physics program. *Journal of Geophysical Research: Oceans* 123(12):8,674–8,687, https://doi.org/10.1002/2018JC013766.

Timmermans, M.-L., S. Cole, and J. Toole. 2012. Horizontal density structure and restratification of the Arctic Ocean surface layer. *Journal of Physical Oceanography* 42 (4):659–668, https://doi.org/10.1175/JPO-D-11-0125.1.

Timmermans, M.-L., A. Proshutinsky, E. Golubeva, J. Jackson, R. Krishfield, M. McCall, G. Platov, J. Toole, W. Williams, T. Kikuchi, and others. 2014. Mechanisms of Pacific Summer Water variability in the Arctic's Central Canada Basin. *Journal of Geophysical Research: Oceans* 119(11):7,523–7,548, https://doi.org/10.1002/2014JC010273.

Tsamados, M., D.L. Feltham, D. Schroeder, D. Flocco, S.L. Farrell, N. Kurtz, S.W. Laxon, and S. Bacon. 2014. Impact of variable atmospheric and oceanic form drag on simulations of Arctic sea ice. *Journal of Physical Oceanography* 44(5):1,329–1,353, https://doi.org/10.1175/JPO-D-13-0215.1.

US Navy. 2014. *U.S. Navy Arctic Roadmap 2014–2030*. Defense Technical Information Center (DTIC), 43 pp.

US Navy. 2019. *Strategic Outlook for the Arctic.* US Department of Defense, 13 pp.

Valkonen, E., J. Cassano, and E. Cassano. 2021. Arctic cyclones and their interactions with the declining sea ice: A recent climatology. *Journal of Geophysical Research: Atmospheres* 126(12), https://doi.org/10.1029/2020JD034366.

Wang, M., and J. Overland. 2015. Projected future duration of the sea-ice-free season in the Alaskan Arctic. *Progress in Oceanography* 136:50–59, https://doi.org/10.1016/j.pocean.2015.01.001.

Wang, X.L., Y. Feng, V.R. Swail, and A. Cox. 2015. Historical changes in the Beaufort-Chukchi-Bering Seas surface winds and waves, 1971–2013. *Journal of Climate* 28(19):7,457–7,469, https://doi.org/10.1175/JCLI-D-15-0190.1.

Williams, T.D., P. Rampal, and S. Bouillon. 2017. Wave-ice interactions in the neXtSIM sea-ice model. *The Cryosphere* 11(5):2,117–2,135, https://doi.org/10.5194/tc-11-2117-2017.

Woodgate, R.A., T. Weingartner, and R. Lindsay. 2010. The 2007 Bering Strait oceanic heat flux and anomalous Arctic sea-ice retreat. *Geophysical Research Letters* 37(1), https://doi.org/10.1029/2009GL041621.

Woodgate, R.A. 2018. Increases in the Pacific inflow to the Arctic from 1990 to 2015, and insights into seasonal trends and driving mechanisms from year-round Bering Strait mooring data. *Progress in Oceanography* 160:124–154, https://doi.org/10.1016/j.pocean.2017.12.007.

Woodgate, R.A., and C. Peralta-Ferriz. 2021. Warming and freshening of the Pacific inflow to the Arctic from 1990–2019 implying dramatic shoaling in Pacific Winter Water ventilation of the Arctic water column. *Geophysical Research Letters* 48(9), e2021GL092528, https://doi.org/10.1029/2021GL092528.

Zhang, D., M.F. Cronin, C. Meinig, J.T. Farrar, R. Jenkins, D. Peacock, J. Keene, A. Sutton, and Q. Yang. 2019. Comparing air-sea flux measurements from a new unmanned surface vehicle and proven platforms during the SPURS-2 field campaign. *Oceanography* 32(2):122–133, https://doi.org/10.5670/oceanog.2019.220.

AUTHORS

Jim Thomson (jthomson@apl.washington.edu) is Senior Principal Oceanographer, **Maddie Smith** is Postdoctoral Scholar, **Kyla Drushka** is Principal Oceanographer, and **Craig Lee** is Senior Principal Oceanographer, all at the Applied Physics Lab, University of Washington, Seattle, WA, USA.